

Transmission of dynamic supercoiling in linear and multi-way branched DNAs and its regulation revealed by a fluorescent G-quadruplex torsion sensor

Ye Xia^{1,2,†}, Ke-wei Zheng^{1,*}, Yi-de He¹, Hong-he Liu¹, Cui-jiao Wen¹, Yu-hua Hao¹ and Zheng Tan^{1,*}

¹State Key Laboratory of Membrane Biology, Institute of Zoology, Chinese Academy of Sciences, Beijing 100101, P.R. China and ²University of Chinese Academy of Sciences, Chinese Academy of Sciences, Beijing 100101, P.R. China

Received February 20, 2018; Revised May 26, 2018; Editorial Decision May 28, 2018; Accepted May 31, 2018

ABSTRACT

DNA supercoiling is an important regulator of gene activity. The transmission of transcription-generated supercoiling wave along a DNA helix provides a way for a gene being transcribed to communicate with and regulate its neighboring genes. Currently, the dynamic behavior of supercoiling transmission remains unclear owing to the lack of a suitable tool for detecting the dynamics of supercoiling transmission. In this work, we established a torsion sensor that quantitatively monitors supercoiling transmission in real time in DNA. Using this sensor, we studied the transmission of transcriptionally generated negative supercoiling in linear and multi-way DNA duplexes. We found that transcription-generated dynamic supercoiling not only transmits along linear DNA duplex but also equally diverges at and proceeds through multi-way DNA junctions. We also show that such a process is regulated by DNA–protein interactions and non-canonical DNA structures in the path of supercoiling transmission. These results imply a transcription-coupled mechanism of dynamic supercoiling-mediated intra- and inter-chromosomal signal transduction pathway and their regulation in DNA.

INTRODUCTION

Genetic information in genomes is maintained and processed by protein–DNA interactions. Several essential cellular processes, for example, replication, transcription, chromatin remodeling and DNA repair, involve translocation of proteins (1), such as helicases (2), DNA polymerases and RNA polymerases (RNAPs) (3,4) on a duplex DNA. The

tracking activity of these motor proteins generates superhelical torsion in the DNA. The torsion under-twist behind and over-twist a DNA helix in front of the moving protein, producing a dynamic transmission of negative and positive supercoiling in two opposite directions. The superhelical state of a DNA is an important determinant of DNA topology and the formation of functional DNA structures such as G-quadruplexes (5–8). It has been demonstrated that transcriptionally generated dynamic negative supercoiling can transmit upward from a transcription start site for several thousand bases and causes a structural change in DNA at a distal upstream region both *in vitro* and *in vivo* (9–11).

On the other hand, gene expression is subjected to the regulation of dynamic conformational changes in DNA (12). The capability of transcriptional supercoiling transmission along and induction of structural changes in a DNA (9–11) implies a transcription-coupled signal transduction pathway right inside a chromosome, making distal communication and regulation possible between neighboring genes (12–14). Genomic DNA is enriched with a variety of structural and functional element, such as secondary structures and protein interacting motifs. A duplex DNA can form several unusual structures, for instance, G-quadruplexes, cruciforms and multi-way junctions. Moreover, a duplex DNA may be bound by various proteins. Thus, the transmission of supercoiling should encounter all these structural features and protein–DNA interactions. So far, supercoiling propagation has been studied by end-point post-reaction protocols that are difficult to capture a fast-moving supercoiling wave, which hampered the investigation of supercoiling dynamics. Therefore, how dynamic supercoiling transmits in different forms of DNAs and how it is regulated in the way of transmission remains unclear.

In this work, we established a torsion sensor that displays in real-time fluorescence enhancement when it captures supercoiling waves originated from a distal DNA site. Using this sensor, we studied the transmission of tran-

*To whom correspondence should be addressed. Tel: +86 10 6480 7259; Fax: +86 10 6480 7099; Email: z.tan@ioz.ac.cn

Correspondence may also be addressed to Ke-wei Zheng. Tel: +86 10 6480 7260; Fax: +86 10 6480 7099; Email: zhengkewei@ioz.ac.cn

†The authors wish it to be known that, in their opinion, the first two authors should be regarded as Joint First Authors.

scriptionally generated negative supercoiling in linear and multi-way DNAs and explored how it was modulated by protein–DNA interactions and non-canonical secondary DNA structures. We demonstrate that bound protein and non-canonical structures both hamper the dynamic supercoiling transmission. We also found that supercoiling wave not only transmits in linear duplex DNA but also splits equally and goes through multi-way DNA junctions. These findings suggest that transcription-coupled signal transduction in DNA may take place within a chromosome and between chromosomes under the modulation by protein–DNA interactions and internal structural elements.

MATERIALS AND METHODS

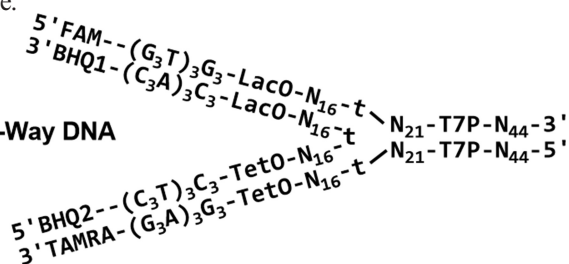
Linear DNA

Linear duplex DNA was prepared by polymerase chain reaction (PCR) using a plasmid template containing a T7 promoter. The forward primer was labeled with an iso-dC and a 6-Fluorescein (FAM) dye at the 5' end and the PCR was conducted in the presence of 2.5 μ M dabcyl-iso-dGTP that pairs only with the iso-dC. The sequences of these DNAs are: GR, 5'-FAM-CA(C₃A)₃C₃-N₂₂₄-T7P-N₈₇; MR, 5'-FAM-CA-N₂₂₄-T7P-N₈₇; GRtruncate, 5'-FAM-CA-(C₃A)₃C₃-N₂₂₄-T7P; GL, 5'-Fam-CA(C₃A)₃C₃-N₉₈-LacO(25bp)-N₁₀₁-T7P-N₈₇; GC, 5'-Fam-CA-(C₃A)₃C₃-N₁₃₆-Cruciform(30bp)-N₅₈-T7P-N₈₇; GG, 5'-FAM-CA-(C₃A)₃C₃-N₁₃₆-(G₃T)₃G₃-N₇₃-T7P-N₈₇; T7P, TAATACGACTCACTATA; LacO, GGAATTGTGAGCGGATAACAATTCC; TetO, TCCCTATCAGTGATAGAGA, where N denotes a random nucleotide.

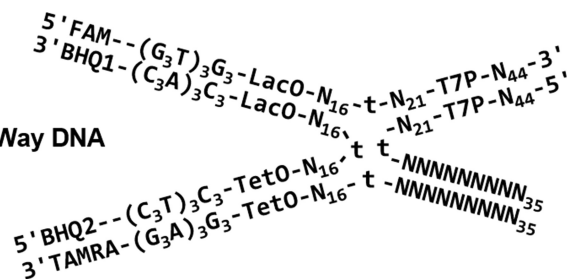
Multi-way DNA

Synthetic oligonucleotides labeled with black-hole quenchers (BHQ1 and BHQ2), or FAM, or without labeling were purchased from Sangon Biotech (Shanghai, China). One oligonucleotide in each set of multi-way DNAs was annealed with a complementary oligonucleotide to create a recessive 3' end which was then labeled by filling-in (15) with a TAMRA-dUTP (Roche, USA). All oligonucleotides were purified by polyacrylamide gel electrophoresis. Multi-way duplex DNA was then prepared by annealing oligonucleotides at 95°C for 5 min followed by a slow cooling to room temperature in a buffer containing 10 mM Tris–HCl (pH 7.9) and 50 mM LiCl in the following scheme.

Three-Way DNA



Four-Way DNA



In vitro transcription and fluorescence spectroscopy

Transcription was carried out with 5 nM linear or 2.5 nM multi-way DNA in a transcription buffer containing 40 mM Tris–HCl, pH 7.9, 40% PEG 200, 75 mM KCl or LiCl if indicated, 10 mM MgCl₂, 10 mM DTT, 2 mM spermidine and 2 mM nucleotide triphosphates (NTPs) (Fermentas, Thermo Scientific, USA) unless otherwise indicated. After 30 min incubation at 37°C, transcription was initiated by an addition of 1 U/ μ l T7 RNAP (Fermentas). Some transcriptions were carried out in the presence of 5 or 20 nM LacI for linear and 10 nM LacI or TetR for multi-way DNA. When transcription was carried out under various concentrations of NTP, the total concentration of Mg²⁺ in the reaction was adjusted as described (16) to maintain a fixed free Mg²⁺ concentration. Fluorescence was recorded over time on a QuantaMaster 40 spectrofluorometer (PTI, USA) with excitation wavelength at 472 nm and emission at 525 nm for FAM or 560 nm and 585 nm for TAMRA. Fluorescence was expressed as fractional increase ΔF , i.e. $(F-F_0)/F_0$, where F and F_0 was the fluorescence at a given and zero time, respectively. Kinetics of fluorescence was analyzed using the following Equation (17)

$$\Delta F = \Delta F_{\max} \cdot \theta, \quad (1)$$

where ΔF was the fractional change in fluorescence, ΔF_{\max} was the maximal value of ΔF and θ represented a two-phase kinetics shown below,

$$\theta = 1 - C \cdot e^{-k_{\text{obs}1}t} - (1 - C) \cdot e^{-k_{\text{obs}2}t}. \quad (2)$$

The parameters, ΔF_{\max} , $k_{\text{obs}1}$, $k_{\text{obs}2}$ and C , were obtained by fitting Equations (1) and (2) to fluorescence time courses. ΔF_{\max} was used as a global parameter in the fitting of each set of experiment. The mean rate constant, k_{obs} , was then calculated as

$$k_{\text{obs}} = C \cdot k_{\text{obs}1} + (1 - C) \cdot k_{\text{obs}2}. \quad (3)$$

DMS footprinting

DMS footprinting of transcribed DNA was performed as previously described (18) using DNA with a FAM label at the upstream 3' end without a quencher.

Expression of LacI and TetR

LacI was amplified from the pET28b by PCR and inserted into the plasmid pMAL-c5X (NEB, UK) between the NcoI and EcoR I sites. The resulting plasmid was again amplified in the *Escherichia coli* strain JM109 (Transgen Biotech, Beijing, China), purified and transformed into *E. coli* strain

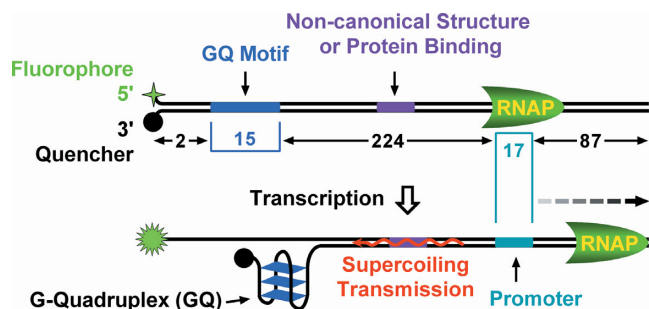


Figure 1. Detection strategy of supercoiling transmission in dsDNA. A fluorophore-quencher pair with a nearby G-quadruplex (GQ) motif ($(G_3T)_3G_3$) is placed at the end opposite to a T7 promoter in a dsDNA with or without protein binding or non-canonical DNA structure-forming motif in between. Without transcription, the fluorophore is quenched by the quencher. Transcription with T7 RNAP generates negative supercoiling that transmits upward and induces a formation of G-quadruplex to pulls apart the fluorophore-quencher pair, leading to an increase in fluorescence. Numbers indicate the size of corresponding DNA elements in base pairs.

BL21. The expressed MBP-tagged LacI was purified by amylose resin affinity chromatography, concentrated by ultrafiltration and stored in a buffer of 50 mM Tris-HCl, pH 7.4, 200 mM NaCl, 50% (v/v) glycerol at -80°C until use. His-tagged TetR protein was cloned from the pCold-I plasmid (Takara, Dalian, China) and processed in the same way as the LacI using nickel affinity chromatography for purification.

RESULTS

Sensing supercoiling transmission and RNA polymerase translocation

Our torsion sensor used a double-stranded DNA (dsDNA) containing a fluorescent dye-quencher pair beside a G-quadruplex forming motif ($(G_3T)_3G_3$) at one end opposite to a T7 promoter at the other (Figure 1). The fluorescence responses to the topological change in the DNA driven by transcription, similar to previous practices employing a dye-quencher pair to detect topological changes in a DNA (19,20). Without transcription, the fluorophore is quenched by a quencher at the opposite DNA strand. Transcription generates negative supercoiling which transmits upward and triggers a formation of G-quadruplex (10). This pulls apart the fluorophore-quencher pair, resulting in an increase in fluorescent emission of the dye. The inclusion of 40% (w/v) PEG 200 in the transcription buffer stabilizes G-quadruplex formation (21). In the meantime, it also elevates the viscosity of the medium to ~ 5 relative to water at 25°C (22) which should enhance the building-up of torsion to drive the formation of G-quadruplex.

Transcription of the DNA in a K^+ solution with T7 RNAP led to a formation of G-quadruplex as judged from the protection of the G_3 tracts to chemical cleavage (Figure 2A). In correlation with this, an increase in fluorescence was observed (Figure 2B, GR/ K^+). Since G-quadruplexes are stabilized by K^+ but not by Li^+ (23), transcription in a Li^+ solution resulted in a much smaller increase in fluorescence (Figure 2B, GR/ Li^+) in comparison with that in K^+ . The small increase in fluorescence in

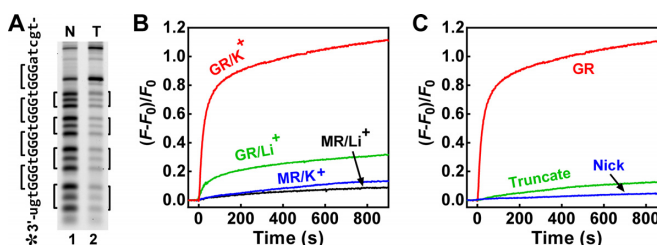


Figure 2. Detection of negative supercoiling transmission in linear dsDNA transcribed by T7 RNAP. (A) G-quadruplex formation in transcribed DNA detected by DMS footprinting. A FAM-labeled dsDNA was not (N) or was (T) transcribed in a K^+ solution before being subjected to DMS footprinting. (B) Increase in fluorescence accompanied by the transcriptional formation of G-quadruplex in DNA. Transcription was initiated by an addition RNAP at zero time in a K^+ - or Li^+ solution. GR, DNA with $(G_3T)_3G_3$; MR, DNA with $(G_3T)_3G_3$ mutant. (C) Fluorescence of truncated and nicked GR DNA transcribed as in (B).

Li^+ likely reflected a formation of a small amount of G-quadruplex stabilized by the PEG 200 in the solution (21). When the $(G_3T)_3G_3$ motif was mutated to abolish its capability of forming a G-quadruplex, the increases in fluorescence both became marginal no matter the transcription was conducted in a K^+ or Li^+ solution (MR/ K^+ and MR/ Li^+).

We further made two modifications to the DNA to verify the connection between the fluorescence response and torsion transmission. When the sequence downstream of the T7 promoter was truncated to prevent RNAP translocation, only marginal fluorescence was detected (Figure 2C, Truncate). When a nick was created on a DNA strand between the promoter and dye-quencher pair, the fluorescent signal barely changed (Figure 2C, Nick). These two results demonstrated that the fluorescence response relied on the tracking activity of the RNAP as well as a continuity of the double DNA helix.

Effect of concentration of NTP on supercoiling transmission

A translocating RNAP grabs an NTP from the medium when it moves to the next nucleotide. The concentration of NTP, therefore, determines how fast an RNAP can move along a DNA template. To assess its effect on supercoiling transmission, we performed transcription under various concentrations of NTP and extracted the kinetics constants by fitting the fluorescent signals to a dual exponential kinetics model (Figure 3A). The derived k_{obs} values as a function of NTP concentration well fitted to an exponential growth function (Figure 3B), indicating that G-quadruplex formation becomes more responsive at higher transcription activity. A prompt increase in k_{obs} occurred when the NTP is over 1.5 mM following an initial slow increase below this concentration. This behavior seems to suggest that an effective transmission of negative supercoiling might require a critical rate of transcription.

G-quadruplex formation induced by single-round transcription

In the aforementioned experiments, DNA was transcribed for multiple rounds. We also carried out experiments in

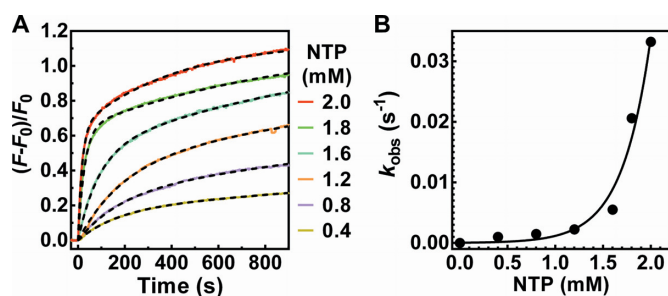


Figure 3. Increase in fluorescence in DNA transcribed with various NTP concentrations. Linear FAM-labeled GR DNA was transcribed as in Figure 2 under the indicated concentrations of NTP. (A) Fluorescence measurements (solid curves) and fittings (dashed curves). (B) Observed rate constant k_{obs} as a function of NTP concentration derived from the fittings in (A). Solid lines are fittings to an exponential growth function.

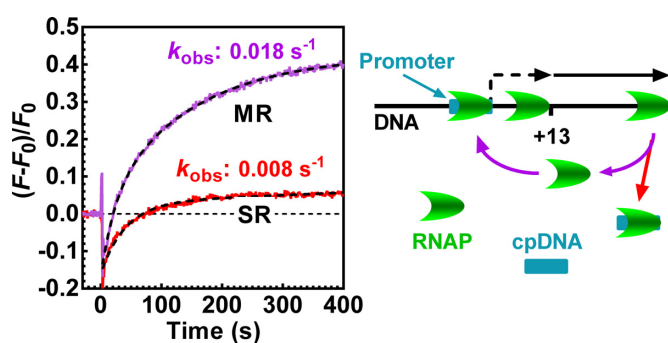


Figure 4. Detection of negative supercoiling transmission in linear dsDNA in single-round transcription. RNAP was loaded onto FAM-labeled DNA and allowed to proceed to engage at +13 in the presence of ATP and GTP (dashed arrow). After a brief incubation, UTP and CTP were supplied together with competitive DNA (cpDNA) for the engaged RNAPs to complete a single-round (SR) full-length transcription (solid arrow, SR curve) before they were released and captured by cpDNA. UTP and CTP were also supplied without cpDNA to permit multi-round (MR) transcription following the first round (MR curve). The concentration of NTP was reduced to 1 mM to minimize the spike at time zero. Change in fluorescence obtained in the absence of RNAP was subtracted as background.

which a DNA could only be transcribed for a single round (24). In these experiments, RNAPs were loaded onto DNAs in the presence of two NTPs to transcribe for 13 nt to get engaged. Then transcription elongation beyond this point was performed by supplying the two remaining NTPs together with a competitive DNA that captured the RNAPs free in solution or released from the DNA, preventing them from re-initiating transcription (Figure 4). Under this condition, a formation of G-quadruplex was also detected by an increase in fluorescence, resulting in a rate constant $k_{\text{obs}} = 0.008 \text{ s}^{-1}$. In the multi-round transcriptions (Figures 2 and 3), the time course of kinetics seemed to be biphasic with a fast initial increase in fluorescence followed by a slow one. However, the second slow phase was not seen in the single-round transcription (Figure 4, SR curve), suggesting that the second slow phase in the multi-round transcriptions might be related to a recycling of RNAPs. By interpolation, the rate constant for multi-round transcription under 1 mM NTP was estimated to be $k_{\text{obs}} = 0.001 \text{ s}^{-1}$ for the observed rate or 0.005 s^{-1} for the faster phase of the biphasic model. In comparison with them, the rate of the

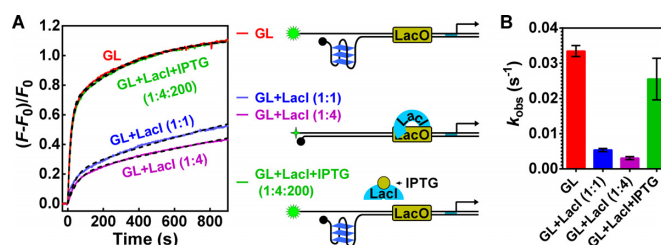


Figure 5. Effect of protein binding on the transmission of negative supercoiling in linear dsDNA. FAM-labeled DNA (GL) containing a LacO element between the T7 promoter and $(G_3T)_3G_3$ motif was transcribed as in Figure 2 in the absence or presence of LacI or LacI and IPTG. (A) Fluorescence measurements (solid curves) and fittings (dashed curves). (B) Observed rate constant k_{obs} (mean \pm range) derived from fittings of two independent experiments.

single-round transcription was greater although the magnitude of fluorescence increment was smaller (Figure 4). This increase in rate could be attributed to a synchronized firing of RNAPs engaged at the DNAs.

Effect of protein–DNA interaction on supercoiling transmission

Most activities associated with genomic DNA involve protein–DNA interactions. Such interaction has been shown to limit supercoiling propagation in plasmids (25,26). The success in monitoring supercoiling transmission prompted us to explore the effect of protein bound to DNA. We placed a lac operator (LacO) in the middle of the DNA and monitored fluorescence in the absence and presence of lac repressor protein (LacI), respectively. As shown in Figure 5, the binding of LacI to the LacO severely suppressed the fluorescence in a concentration-dependent manner, leading to a dramatic decrease in the k_{obs} . The suppression largely diminished when isopropyl-beta-D-thiogalactopyranoside (IPTG), an allosteric inducer of lacI, was added to inactivate the LacI (GL+LacI+IPTG). These results demonstrated that the transmission of supercoiling is suppressed by protein–DNA interaction in the way of torsion transmission.

Effect of cruciform and G-quadruplex on supercoiling transmission

Secondary structures, like cruciforms and G-quadruplexes, are abundant in the human genome (15,27–30). We then studied how such structures would affect supercoiling transmission, a question that has not yet been addressed previously. We placed a cruciform and G-quadruplex motif in the middle of the DNA, respectively, and monitored fluorescence in comparison with that of a control DNA containing no structure-forming motif at the corresponding position. Both the cruciform and G-quadruplex motif led to a decrease in fluorescence and reduction in k_{obs} (Figure 6), indicating that the two structures both suppressed the transmission of supercoiling with the latter being more effective. It is very common to find tandem G-quadruplex motifs in human genes. Our results thus imply that in such cases the structural responses of these G-quadruplex motifs to tran-

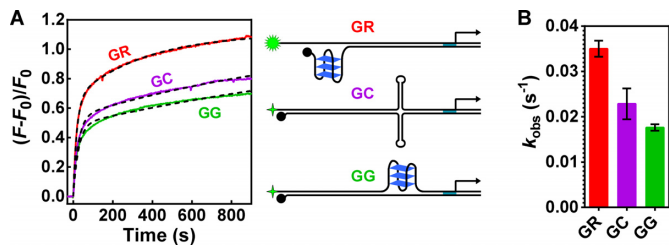


Figure 6. Effect of cruciform and G-quadruplex on the transmission of negative supercoiling in linear dsDNA. A cruciform (GC) or a G-quadruplex (GG) forming motif was placed between the T7 promoter and $(G_3T)_3G_3$ motif. The two DNAs had the same length as the control DNA (GR). DNAs were transcribed as in Figure 2. (A) Fluorescence measurements (solid curves) and fittings (dashed curves). (B) Observed rate constant k_{obs} (mean \pm range) derived from fittings of two independent experiments.

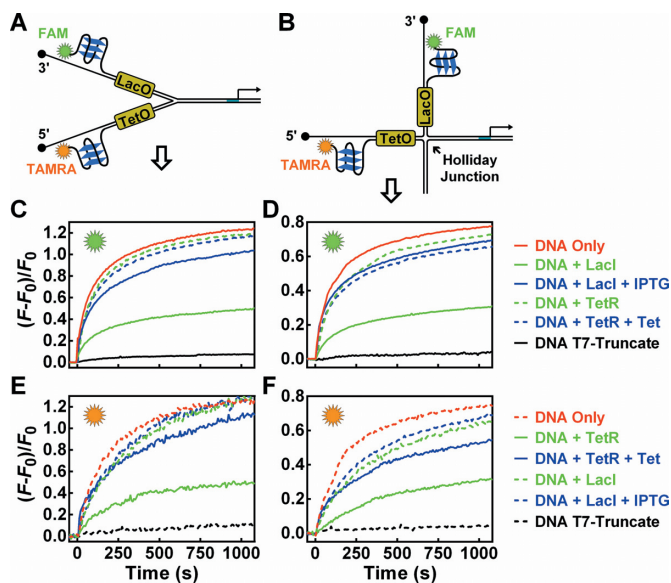


Figure 7. Detection of negative supercoiling transmission in three- and four-way dsDNAs. (A and B) Scheme of DNA arrangement. A protein binding site LacO or TetO was placed in the indicated sensing arm with the indicated fluorescent dye (FAM or TAMRA). (C–F) Fluorescence measurements. DNA was transcribed as in Figure 2 in the absence or presence of the indicated DNA binding proteins and their inhibitors. Fluorescence indicated by a solid line in (C) or (D) was measured simultaneously with that indicated by a dashed line of the same color in (E) or (F) and *vice versa*.

scription will depend on their position relative to that of a transcription event.

Transmission of supercoiling through multi-way junctions

The transmission of supercoiling through the cruciform suggested a capability for the dynamic supercoiling to pass a multi-way junction, a structure that often forms in genetic processes like DNA recombination and repair (31,32). To test this anticipation, we first made a three-way branched DNA duplex by annealing three individual DNA strands half-complementary to each other. It contained a T7 promoter in one arm and a $(G_3T)_3G_3$ motif in the other two with either a FAM or TAMRA dye (Figure 7A). Transcription led to a rise in fluorescence of both dyes, indicating that

the transcription generated supercoiling passed the three-way junction to reach the two $(G_3T)_3G_3$ motifs, respectively (Figure 7C and E, red curve). The magnitude of fluorescence increase of the two dyes was similar to each other, suggesting that the supercoiling wave diverged into the two sensing arms without bias.

The supercoiling transmission was further tested for its regulation by protein binding in this branched DNA as in Figure 5. When the LacO in the FAM bearing arm was bound by LacI, the FAM fluorescence was dramatically reduced (Figure 7C, solid green versus red curve) which was also rescued as expected by IPTG that inactivates LacI (solid blue curve). In contrast, an inclusion of TetR, a TetO binding protein targeting the TetO on the other sensing arm, or its allosteric inhibitor Tet in the transcription resulted in little change in the fluorescence of the FAM (dashed green and blue curves). The TAMRA dye on the other sensing arm responded similarly with a specificity to TetO (Figure 7E). Its fluorescence (dashed red curve) was dramatically suppressed by the binding of TetR to the TetO (solid green curve) between the $(G_3T)_3G_3$ motif and the junction and rescued by Tet that inhibits the TetR (solid blue curve).

We further examined a four-way DNA structure known as Holliday junction (Figure 7B, D and F) in a similar architecture. The results obtained (Figure 7D and F) were also similar to those from the three-way DNA, indicating a transmission of supercoiling through the four-way junction. Both dyes in the two sensing arms showed an increase in fluorescence in response to transcription at the transcribing arm (red curve), which again was both suppressed by the specific protein bound to their corresponding targets (solid green curve) and rescued by the inactivation of the binding protein (solid blue curve). In addition, protein binding to irrelevant arms only led to marginal changes in the fluorescence of the dyes (dashed green and blue curves). The similar magnitudes of fluorescence responses to transcription (red curves) again supported an equal divergence of supercoiling wave into the three DNA arms. One un-labeled arm was not analyzed since it is topologically symmetric to the arm labeled with the FAM dye to which the same conclusion applies.

DISCUSSION

In summary, we established a DNA torsion sensor to monitor the transmission of negative supercoiling in transcribed DNA based on a formation of a G-quadruplex. Using this device, our work revealed two major findings regarding the transmission of supercoiling and its regulation in DNA. First, the dynamic supercoiling wave not only transmits through linear DNA duplex (Figures 2 and 3) but also split up equally and passes through multi-way DNA junctions (Figure 7). This property implies that a transcription-coupled signal transduction may occur either within a chromosome or between chromosomes when, for instance, a recombination takes place in the neighborhood of a transcribing gene. Transcription-associated recombination is a conserved feature in all cellular organisms, ranging from bacteria to mammals (33). Transcription is also known to stimulate homologous recombination in mammalian cells (34).

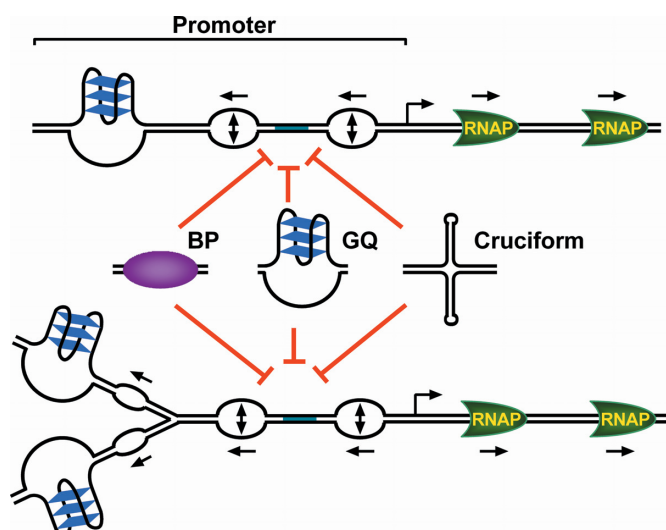


Figure 8. Proposed model of transmission of transcription-generated negative supercoiling, distal induction of G-quadruplex formation and regulation in the transmission path. Transcription fires backward waves of negative supercoiling that opens nucleotides pairing (dual-headed arrows). The opening may trigger a formation of G-quadruplex when it passes a G-quadruplex-forming motif. Propagation of mechanical wave relies on deformation of the medium. A bound protein (BP), a G-quadruplex (GQ) and cruciform may all suppress the deformation and, as a result, reduce the propagation of supercoiling through them.

Our results, therefore, suggest a potential role of supercoiling transmission in connecting gene expression and recombination.

Secondly, the dynamic wave of supercoiling transmission in a DNA is modulated by DNA–protein interactions and internal non-canonical DNA structures (Figures 5–7) in the path of transmission, which may regulate transcriptional signal transduction along a DNA helix. This regulation may participate in the coordination of gene activities. It is known that dynamic modification of DNA supercoiling regulates gene expression (12,13,35). Gene expression is not an isolated activity, but in many cases coordinates among genes in cells (36). In particular, functionally related genes are often clustered in close proximity to each other on a chromosome. It is assumed that the interactions between the transcriptional machineries of neighboring genes play a fundamental role in coordinating gene expression (37). The communication through supercoiling transmission in a DNA may be one of the means to coordinate.

The propagation of mechanical torsion, like other mechanical waves, involves deformation of the medium. A DNA helix can be considered as a one-dimensional elastic medium at a macroscopic level. Transcriptionally generated transient torsion is large enough to disrupt DNA helix into single-stranded form at the upstream of active promoters (11). The disruption of base-pairing provides a chance for G-quadruplexes to form (Figure 8). The binding of a protein to DNA should impose restrictions to the deformation of the DNA to suppress the torsion propagation. For the two DNA binding proteins we used, LacI is a tetramer containing two dimeric DNA-binding subunits (38). While one of its subunits could specifically bind to the major groove of its target DNA, the other subunit may non-specifically bind

the DNA (39), inducing DNA looping; TetR is a homodimeric protein that binds to the major groove of its target DNA (40). In either case, the deformation of the DNA helix is constrained by the interaction between the protein and the two DNA strands. An increased friction from the protein is also expected to limit the DNA deformation. As to the two non-canonical structures, its suppression on torsion transmission might be caused by the disruption of continuity of the DNA helix and the constraint of deformation by the formation of a more rigid structure.

Since a promoter is where transcription is initiated, the upward transmission of supercoiling and subsequent formation of G-quadruplex establishes a feedback of transcription activity to its promoter for self-regulation. G-quadruplex-forming motifs are significantly enriched in the promoter region of genes in warm-blooded animals (10) which are subject to the induction by downstream transcriptions. Our data show that a single-round of transcription is able to induce a formation of G-quadruplex with a certain probability (Figure 4). The NTP concentration-dependence of G-quadruplex formation (Figure 3) implies a probability of G-quadruplex formation in positive correlation to transcription activity under the control of DNA–protein interactions and non-canonical DNA structures. A formation of G-quadruplex will then modulate the way a promoter interacts with RNAP or transcription-binding factor which in return affect the subsequent transcription of a gene.

Our torsion sensor is expected to provide a useful tool for monitoring supercoiling transmission in DNA. Its real-time capability offers kinetic insight that is normally unavailable or difficult to derive from conventional methods. Since the torsion sensor is implemented on a coupling of four-event cascade of protein translocation → physical torsion transmission → G-quadruplex formation → fluorophore-quencher separation, it can also be tuned to perform real-time study on a number of DNA associated activities in general, namely DNA tracking, supercoiling transmission, protein–DNA interaction, and G-quadruplex formation, simply by arranging desired functional elements in the DNA. For example, translocation of different motor proteins can be studied using different promoters or recognition sequences. Protein–DNA interaction can be investigated by arranging appropriate recognition motifs. The transcriptional G-quadruplex formation can be detected in different G-quadruplex-forming motifs.

FUNDING

National Natural Science Foundation of China, grant numbers 21672212, 31470783, 21432008. Funding for open access charge: National Natural Science Foundation of China.

Conflict of interest statement. None declared.

REFERENCES

1. Bujalowski, W. (2001) Motor Proteins in DNA Metabolism: Structures and Mechanisms. *Encyclopedia of Life Sciences*. John Wiley & Sons, Ltd.
2. Yu, J., Ha, T. and Schulten, K. (2007) How directional translocation is regulated in a DNA helicase motor. *Biophys. J.*, **93**, 3783–3797.
3. Kornberg, R.D. (2007) The molecular basis of eukaryotic transcription. *Proc. Natl. Acad. Sci. U.S.A.*, **104**, 12955–12961.

4. Gelles, J. and Landick, R. (1998) RNA polymerase as a molecular motor. *Cell*, **93**, 13–16.
5. Sun, D. and Hurley, L.H. (2009) The importance of negative superhelicity in inducing the formation of G-quadruplex and i-motif structures in the c-Myc promoter: implications for drug targeting and control of gene expression. *J. Med. Chem.*, **52**, 2863–2874.
6. Lv, B., Li, D., Zhang, H., Lee, J.Y. and Li, T. (2013) DNA gyrase-driven generation of a G-quadruplex from plasmid DNA. *Chem. Commun. (Camb.)*, **49**, 8317–8319.
7. Selvam, S., Koirala, D., Yu, Z. and Mao, H. (2014) Quantification of topological coupling between DNA superhelicity and G-quadruplex formation. *J. Am. Chem. Soc.*, **136**, 13967–13970.
8. Sekibo, D.A.T. and Fox, K.R. (2017) The effects of DNA supercoiling on G-quadruplex formation. *Nucleic Acids Res.*, **45**, 12069–12079.
9. Kouzine, F., Gupta, A., Baranello, L., Wojtowicz, D., Ben-Aissa, K., Liu, J., Przytycka, T.M. and Levens, D. (2013) Transcription-dependent dynamic supercoiling is a short-range genomic force. *Nat. Struct. Mol. Biol.*, **20**, 396–403.
10. Zhang, C., Liu, H.H., Zheng, K.W., Hao, Y.H. and Tan, Z. (2013) DNA G-quadruplex formation in response to remote downstream transcription activity: long-range sensing and signal transducing in DNA double helix. *Nucleic Acids Res.*, **41**, 7144–7152.
11. Kouzine, F., Liu, J., Sanford, S., Chung, H.J. and Levens, D. (2004) The dynamic response of upstream DNA to transcription-generated torsional stress. *Nat. Struct. Mol. Biol.*, **11**, 1092–1100.
12. Levens, D., Baranello, L. and Kouzine, F. (2016) Controlling gene expression by DNA mechanics: emerging insights and challenges. *Biophys. Rev.*, **8**, 259–268.
13. Fogg, J.M., Randall, G.L., Pettitt, B.M., Summers, W.L., Harris, S.A. and Zechiedrich, L. (2012) Bullied no more: when and how DNA shoves proteins around. *Q. Rev. Biophys.*, **45**, 257–299.
14. Sobetzko, P. (2016) Transcription-coupled DNA supercoiling dictates the chromosomal arrangement of bacterial genes. *Nucleic Acids Res.*, **44**, 1514–1524.
15. Zheng, K.W., Xiao, S., Liu, J.Q., Zhang, J.Y., Hao, Y.H. and Tan, Z. (2013) Co-transcriptional formation of DNA:RNA hybrid G-quadruplex and potential function as constitutional cis element for transcription control. *Nucleic Acids Res.*, **41**, 5533–5541.
16. Marks, P.W. and Maxfield, F.R. (1991) Preparation of solutions with free calcium concentration in the nanomolar range using 1,2-bis(o-aminophenoxy)ethane-N,N,N',N'-tetraacetic acid. *Anal. Biochem.*, **193**, 61–71.
17. Zhao, Y., Zhang, J.Y., Zhang, Z.Y., Tong, T.J., Hao, Y.H. and Tan, Z. (2017) Real-time detection reveals responsive cotranscriptional formation of persistent intramolecular DNA and intermolecular DNA:RNA hybrid G-quadruplexes stabilized by R-Loop. *Anal. Chem.*, **89**, 6036–6042.
18. Zheng, K.W., Chen, Z., Hao, Y.H. and Tan, Z. (2010) Molecular crowding creates an essential environment for the formation of stable G-quadruplexes in long double-stranded DNA. *Nucleic Acids Res.*, **38**, 327–338.
19. Jude, K.M., Hartland, A. and Berger, J.M. (2013) Real-time detection of DNA topological changes with a fluorescently labeled cruciform. *Nucleic Acids Res.*, **41**, e133.
20. Gu, M., Berrido, A., Gonzalez, W.G., Miksovska, J., Chambers, J.W. and Leng, F. (2016) Fluorescently labeled circular DNA molecules for DNA topology and topoisomerases. *Sci. Rep.*, **6**, 36006.
21. Kan, Z.Y., Yao, Y., Wang, P., Li, X.H., Hao, Y.H. and Tan, Z. (2006) Molecular crowding induces telomere G-quadruplex formation under salt-deficient conditions and enhances its competition with duplex formation. *Angew. Chem. Int. Ed. Engl.*, **45**, 1629–1632.
22. Kozler, N., Kuttner, Y.Y., Haran, G. and Schreiber, G. (2007) Protein-protein association in polymer solutions: from dilute to semidilute to concentrated. *Biophys. J.*, **92**, 2139–2149.
23. Hardin, C.C., Perry, A.G. and White, K. (2000) Thermodynamic and kinetic characterization of the dissociation and assembly of quadruplex nucleic acids. *Biopolymers*, **56**, 147–194.
24. Zhang, J.Y., Zheng, K.W., Xiao, S., Hao, Y.H. and Tan, Z. (2014) Mechanism and manipulation of DNA:RNA hybrid G-quadruplex formation in transcription of G-rich DNA. *J. Am. Chem. Soc.*, **136**, 1381–1390.
25. Leng, F., Chen, B. and Dunlap, D.D. (2011) Dividing a supercoiled DNA molecule into two independent topological domains. *Proc. Natl. Acad. Sci. U.S.A.*, **108**, 19973–19978.
26. Zheng, K.W., He, Y.D., Liu, H.H., Li, X.M., Hao, Y.H. and Tan, Z. (2017) Superhelicity constrains a localized and R-loop-dependent formation of G-quadruplexes at the upstream region of transcription. *ACS Chem. Biol.*, **12**, 2609–2618.
27. Brazda, V., Laister, R.C., Jagelska, E.B. and Arrowsmith, C. (2011) Cruciform structures are a common DNA feature important for regulating biological processes. *BMC Mol. Biol.*, **12**, 33.
28. Huppert, J.L. and Balasubramanian, S. (2005) Prevalence of quadruplexes in the human genome. *Nucleic Acids Res.*, **33**, 2908–2916.
29. Todd, A.K., Johnston, M. and Neidle, S. (2005) Highly prevalent putative quadruplex sequence motifs in human DNA. *Nucleic Acids Res.*, **33**, 2901–2907.
30. Li, X.M., Zheng, K.W., Zhang, J.Y., Liu, H.H., He, Y.D., Yuan, B.F., Hao, Y.H. and Tan, Z. (2015) Guanine-vacancy-bearing G-quadruplexes responsive to guanine derivatives. *Proc. Natl. Acad. Sci. U.S.A.*, **112**, 14581–14586.
31. Altona, C., Pikkemaat, J.A. and Overmars, F.J. (1996) Three-way and four-way junctions in DNA: a conformational viewpoint. *Curr. Opin. Struct. Biol.*, **6**, 305–316.
32. Lilley, D.M. (2000) Structures of helical junctions in nucleic acids. *Q. Rev. Biophys.*, **33**, 109–159.
33. Aguilera, A. (2002) The connection between transcription and genomic instability. *EMBO J.*, **21**, 195–201.
34. Nickoloff, J.A. and Reynolds, R.J. (1990) Transcription stimulates homologous recombination in mammalian cells. *Mol. Cell. Biol.*, **10**, 4837–4845.
35. Ma, J. and Wang, M. (2014) Interplay between DNA supercoiling and transcription elongation. *Transcription*, **5**, e28636.
36. Komili, S. and Silver, P.A. (2008) Coupling and coordination in gene expression processes: a systems biology view. *Nat. Rev. Genet.*, **9**, 38–48.
37. Boldogkoi, Z. (2012) Transcriptional interference networks coordinate the expression of functionally related genes clustered in the same genomic loci. *Front. Genet.*, **3**, 122.
38. Lewis, M., Chang, G., Horton, N.C., Kercher, M.A., Pace, H.C., Schumacher, M.A., Brennan, R.G. and Lu, P. (1996) Crystal structure of the lactose operon repressor and its complexes with DNA and inducer. *Science*, **271**, 1247–1254.
39. Kalodimos, C.G., Biris, N., Bonvin, A.M., Levandoski, M.M., Guennegues, M., Boelens, R. and Kaptein, R. (2004) Structure and flexibility adaptation in nonspecific and specific protein-DNA complexes. *Science*, **305**, 386–389.
40. Ramos, J.L., Martinez-Bueno, M., Molina-Henares, A.J., Teran, W., Watanabe, K., Zhang, X., Gallegos, M.T., Brennan, R. and Tobes, R. (2005) The TetR family of transcriptional repressors. *Microbiol. Mol. Biol. Rev.*, **69**, 326–356.